

**P5.14** SUMMERTIME NORTH PACIFIC CLOUD FEEDBACKS INFERRED FROM SYNOPTIC-SCALE DYNAMIC AND THERMODYNAMIC RELATIONSHIPS

Joel R. Norris\* and Sam F. Iacobellis

Scripps Institution of Oceanography, University of California, San Diego

## 1. INTRODUCTION

Clouds have a large impact on Earth's radiation budget because they typically reflect more shortwave (SW) radiation and emit less longwave (LW) radiation to space than does the unobscured surface. Despite their importance, the sign and magnitude of cloud feedbacks on the climate system are some of the largest uncertainties of future climate change. Clouds over midlatitude oceans during summer are of particular interest since they produce net cloud radiative forcing that is more negative than anywhere else on Earth (Harrison et al. 1990). Synoptic ascent generates thick frontal cloudiness that can reflect as much as  $200 \text{ W m}^{-2}$  of SW radiation more than clear sky. Extensive stratocumulus cloudiness under synoptic descent following the cold front typically reflects  $100 \text{ W m}^{-2}$  more than clear sky (Weaver and Ramanathan 1997). In addition to vertical motion, advection over the sea surface temperature (SST) gradient separating subpolar and subtropical gyres substantially changes low-level cloud properties. The climatological distribution of surface-observed low cloud types suggests poleward advection of warm subtropical air over colder water causes stratification of the near-surface layer that leads to the suppression of cumulus clouds and eventually the formation of fog and stratus. Equatorward advection of midlatitude stratocumulus over warmer water causes decoupling of the boundary layer and a transition to cumulus (Norris 1998a; Norris 1998b).

The strategy of the present study is to separately characterize dynamical and thermodynamical effects on cloud properties using a method similar to that of Bony et al. (2004). The region and time period of the investigation is the North Pacific during 1983-2001 since insolation and consequently cloud reflection are large at this time of year. Daily values of cloud amount, cloud optical thickness ( $\tau$ ), and cloud top pressure (CTP) are averaged within small intervals of mid-tropospheric vertical motion and near-surface meridional wind to determine how synoptic forcing in conjunction with advection over the SST gradient controls cloud properties. The cloud data in each vertical motion and meridional wind interval are then subdivided into terciles of anomalously cold or warm SST and anomalously strong or weak lower tropospheric static stability. The average of the data within the middle terciles represents "normal" conditions, and the difference between the averages of the upper and lower terciles represents how cloud properties change with temperature or stratification.

This procedure effectively calculates the partial derivatives of cloud fraction,  $\tau$ , and CTP with respect to vertical motion, meridional wind, SST/atmospheric temperature, and static stability. Long-term cloud feedbacks on the climate system may be inferred from these synoptic-scale relationships.

## 2. DATA

The ISCCP D1 product provides values of cloud fraction, mean visible  $\tau$ , and mean CTP in  $2.5^\circ \times 2.5^\circ$  grid boxes every three hours (Rossow et al. 1996; Rossow and Schiffer 1999). Although ISCCP data are available every 3 hours, only 00 UTC values are used in order to match the 6-hourly reanalysis data at a local time of day (noon over the central North Pacific) when the solar zenith angle is small and cloud retrievals have less error. Impacts of cloud properties on the top-of-atmosphere radiation budget are assessed using daily mean values of SW, LW, and net cloud radiative forcing (CRF) in  $2.5^\circ \times 2.5^\circ$  grid boxes previously used in Norris and Weaver (2001) and originally obtained from the Earth Radiation Budget Experiment (ERBE) (Barkstrom et al. 1989). These data are available for 1985-89. Radiative flux is defined as positive downwards such that SW CRF is negative and LW CRF is positive.

The NCEP/NCAR Reanalysis I provides values of vertical motion, horizontal winds, and temperature on standard pressure levels at  $2.5^\circ \times 2.5^\circ$  grid spacing every six hours (Kalnay et al. 1996). Even though vertical motion is diagnosed by the model rather than directly measured, Norris and Weaver (2001) found negligible difference between statistical cloud relationships based on NCEP/NCAR Reanalysis vertical motion or ECMWF Reanalysis vertical motion. Monthly mean SST values are obtained from version 2 of the Reynolds OI dataset, a combination of in situ and satellite measurements of SST (Reynolds 2002). Lower tropospheric static stability (LTS) is defined as  $\theta_{700} - \theta_{SST}$ , where  $\theta_{700}$  is the potential temperature at the 700-hPa level and  $\theta_{SST}$  is the potential temperature at the surface (calculated from SST and SLP).

## 3. THERMODYNAMICAL COMPOSITES

Vertical motion, near-surface meridional wind, SST, and LTS are useful proxies for many of the actual processes generating cloud condensate that are not accurately observed or modeled by the reanalysis. Vertical motion is closely tied to the advective tendency of total water mixing ratio, and meridional wind, SST, and LTS greatly influence boundary layer turbulent mixing and entrainment. The dependence of cloud properties on vertical motion, meridional wind, SST, and LTS can be determined by dividing each parameter into

\* Corresponding author address: Joel R. Norris, Scripps Institution of Oceanography, La Jolla, CA 92093-0224; e-mail: jnorris@ucsd.edu.

multiple intervals and averaging daily cloud values within the intervals. For simplicity, 500 hPa pressure vertical velocity ( $\omega_{500}$ ) and 1000 hPa meridional wind component ( $v_{1000}$ ) are the only dynamical parameters considered. The different effects on cloud properties of vertically uniform changes in temperature and changes in vertical stratification are examined by holding LTS constant and letting SST vary in the first case and holding SST constant and letting LTS vary in the second case.

Following the two-variable composite technique of Ringer and Allan (2004), dynamical composites of cloud amount,  $\tau$ , and CTP were created by classifying every ISCCP value within the region 35-45°N, 160-195°E during July 1983-2001 into 50 hPa day<sup>-1</sup> intervals of  $\omega_{500}$  and 2.5 m s<sup>-1</sup> intervals of  $v_{1000}$ . ISCCP data in each bi-interval were further classified into terciles of SST anomalies and terciles of LTS anomalies. Use of anomalies was required by the large climatological meridional variation of SST and LTS that would otherwise cause a strong geographical bias in the results. Cloud amount,  $\tau$ , and CTP for each  $\omega_{500}/v_{1000}$  bi-interval under “normal” conditions were determined by averaging ISCCP values corresponding to the middle SST and middle LTS terciles.

Effects of a vertically uniform increase in temperature on cloud properties were estimated by subtracting the average of ISCCP values corresponding to the lower SST and middle LTS terciles from the average corresponding to the upper SST and middle LTS terciles. Statistical significance was determined by first calculating the difference between averages of two sets of randomly chosen values (with replacement) within each  $\omega_{500}/v_{1000}$  bi-interval. The number of values in each random set was the same as the number of values contributing to the upper SST/middle LTS or lower SST/middle LTS terciles. This was repeated one thousand times, and the random differences were placed in ascending order. Composite differences were then deemed statistically significant if they were smaller than the 26<sup>th</sup> or larger than the 975<sup>th</sup> random difference. Effects of increasing LTS were estimated by subtracting the average of lower LTS and middle SST terciles from the average of upper LTS and middle SST terciles.

Figure 1 displays composite ISCCP cloud properties for “normal” SST and LTS. Cloud amount is nearly 100% except when vertical motion is downward and meridional wind is northward (Fig. 1a). This downward/northward quadrant corresponds to a region with enhanced frequency of clear sky occurring ahead of an extratropical cyclone where warm air is advected northward over cold water and the resulting stratification limits upward moisture fluxes and suppresses cloud formation.  $\tau$  is also least in the downward/northward quadrant (Fig. 1b). CTP decreases and  $\tau$  increases as vertical motion becomes more negative (Fig. 1bc), consistent with the generation of thick clouds with high tops by synoptic ascent. It is important to keep in mind that  $\omega_{500}/v_{1000}$  bi-intervals do not occur with equal frequency. Figure 1d indicates that  $\omega_{500}$  and  $v_{1000}$  are close to normally distributed, with weak upward and

northward motion happening most often. The linear correlation coefficient between  $\omega_{500}$  and  $v_{1000}$  is  $-0.42$ .

Figure 2 shows composite SW, LW, and net CRF obtained from daily ERBE data during the 1985-89 and calculated in the same manner as for Fig. 1. Note that less data are available since the ERBE time period is only one fourth as long as the ISCCP time period. Consistent with Fig. 1, SW CRF is greatest where cloud amount and  $\tau$  are greatest and least where they are least (Fig. 2a). Similarly, the magnitude of LW CRF inversely varies with CTP (Fig. 2b). Net CRF is always negative because SW CRF is always larger than LW CRF in this region. The most negative values of net CRF occur with strong ascent, and the least negative values occur in the downward/northward quadrant (Fig. 2c).

Table 1 lists mean cloud properties, SST, and LTS associated with middle SST and LTS terciles calculated by averaging over the distributions in Figs. 1 and 2 with weighting by the frequency of occurrence of each  $\omega_{500}/v_{1000}$  bi-interval ( $\tau$  and CTP were additionally weighted by cloud amount in each bi-interval). For completeness, properties averaged over regions north (45-55°N, 160-195°E) and south (25-35°N, 160-195°E) of the SST gradient are also included. Magnitudes of cloud amount,  $\tau$ , CTP, SW CRF, and net CRF increase from south to north. Despite having the smallest value of CTP, the southern region does not have the largest value of LW CRF because most of the high clouds are transmissive cirrus. Although not shown, the relative distributions of cloud properties with respect to  $\omega_{500}$  and  $v_{1000}$  in the southern and northern regions are generally similar to those in the central region (displayed in Figs. 1 and 2). The largest latitudinal differences occur in the downward/northward quadrant, where the relative minima in cloud amount and  $\tau$  do not occur in the northern region due to the formation of fog. These relative minima are larger in the southern region than in the central region. Some thin cirrus clouds also occur in the downward/northward quadrant of the southern region. The fact that cloud properties in an  $\omega_{500}/v_{1000}$  bi-interval vary with latitude indicates that the instantaneous dynamical state is not a complete proxy for the meteorological processes controlling cloudiness, but analyzing latitude zones separately will mitigate the influence of these unaddressed processes.

Figure 3 displays statistically significant differences between ISCCP cloud properties composited on upper and lower SST terciles for the 35-45°N region. The data were restricted to the middle tercile of LTS in both cases to exclude effects resulting from changes in atmospheric stratification. Thus, the cloud differences result from identical temperature changes at 700 hPa and the surface. Cloud amount and  $\tau$  are generally lower and CTP is generally higher for warmer conditions. Due to the shortness of the ERBE time period, very few  $\omega_{500}/v_{1000}$  bi-intervals have statistically significant CRF differences and are therefore not displayed. Table 2 lists differences in ISCCP and ERBE cloud properties averaged over all  $\omega_{500}/v_{1000}$  bi-intervals with weighting by frequency. Note that the cloud

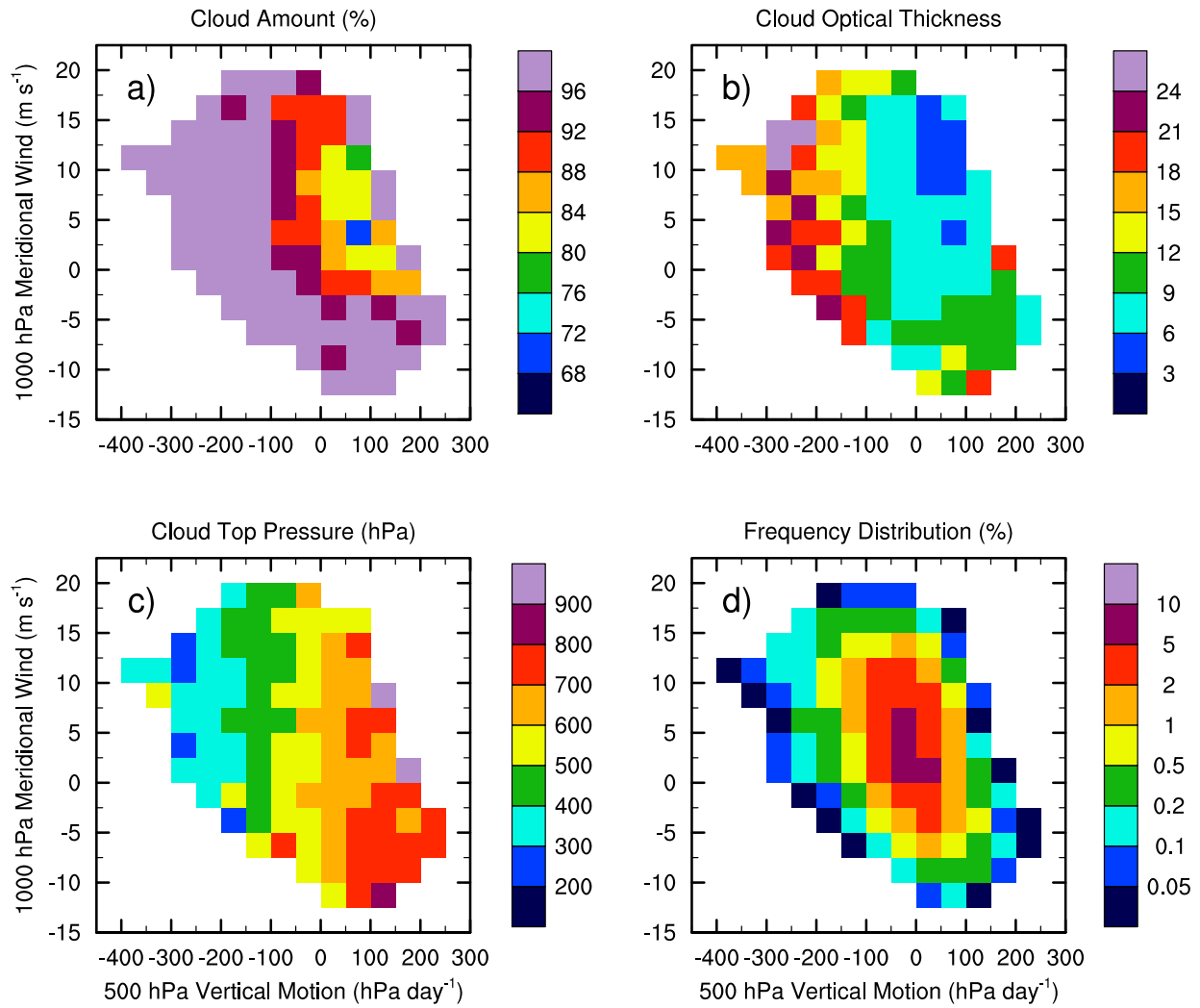


Fig. 1. Composite (a) ISCCP cloud amount (%), (b) ISCCP  $\tau$ , (c) ISCCP CTP (hPa), and (d) frequency of occurrence for  $\omega_{500}/V_{1000}$  bi-intervals in the region 35-45°N, 160-195°E during July 1983-2001. Averages are calculated only for those values associated with the middle terciles of standardized SST anomalies and standardized LTS anomalies. Note that positive values of  $\omega_{500}$  correspond to downward motion.

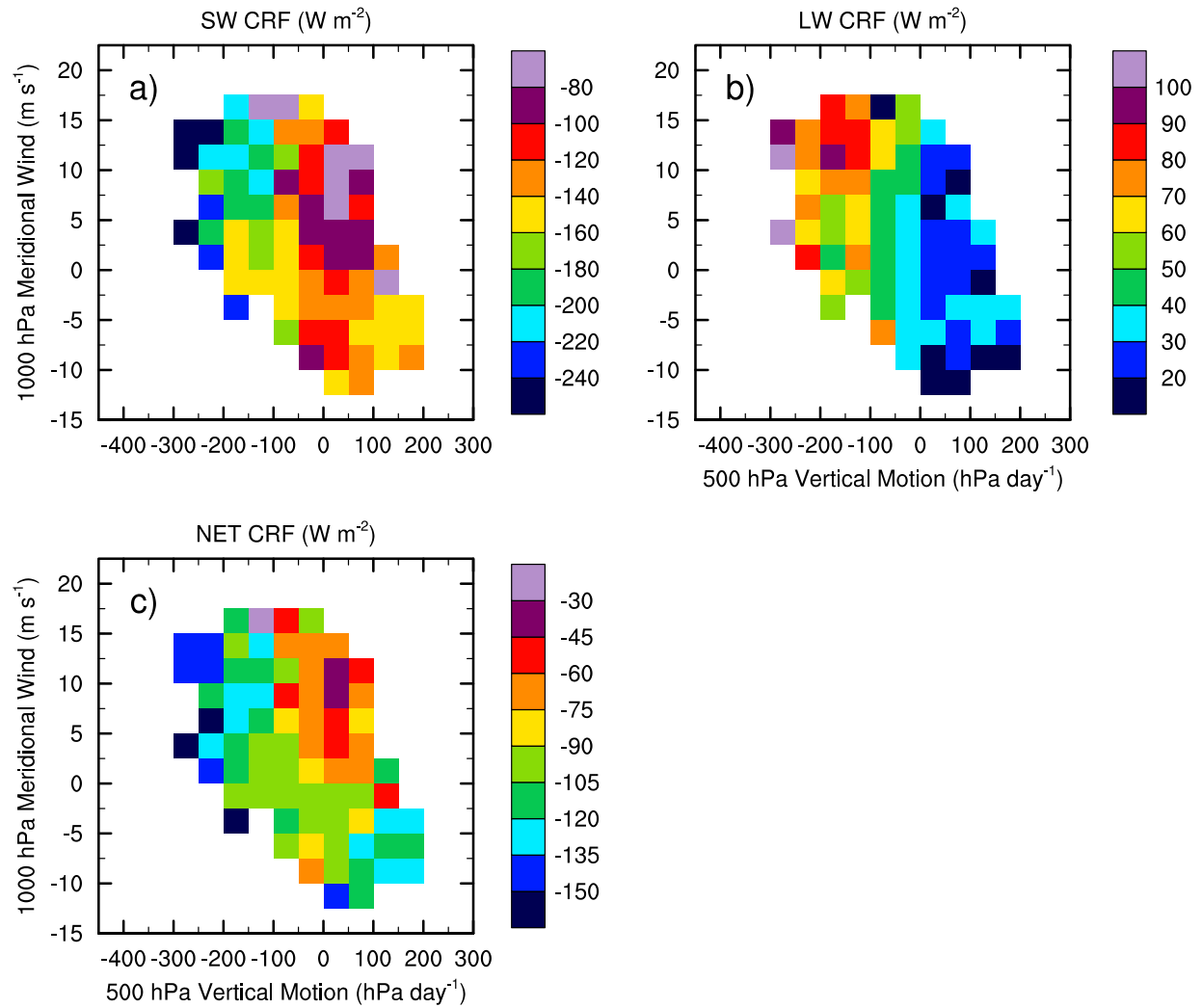


Fig. 2. As in Fig. 1, except for ERBE (a) SW CRF, (b) LW CRF, and (c) net CRF during July 1985-89.

Table 1. Average properties for middle SST and LTS terciles.\*

Latitude Region	Cloud Amount (%)	$\tau$	CTP (hPa)	SW CRF ( $\text{W m}^{-2}$ )	LW CRF ( $\text{W m}^{-2}$ )	Net CRF ( $\text{W m}^{-2}$ )	SST ( $^{\circ}\text{C}$ )	LTS (K)
45-55 $^{\circ}$ N	98.1	10.8	624	-156	30	-126	8.8	23.4
35-45 $^{\circ}$ N	91.0	8.2	589	-120	38	-83	16.6	20.2
25-35 $^{\circ}$ N	60.6	3.1	513	-44	27	-18	25.6	13.3

\* Averaged over 165-190 $^{\circ}$  E during 1983-2001 (cloud amount,  $\tau$ , CTP, SST, LTS) or 1985-89 (CRF).

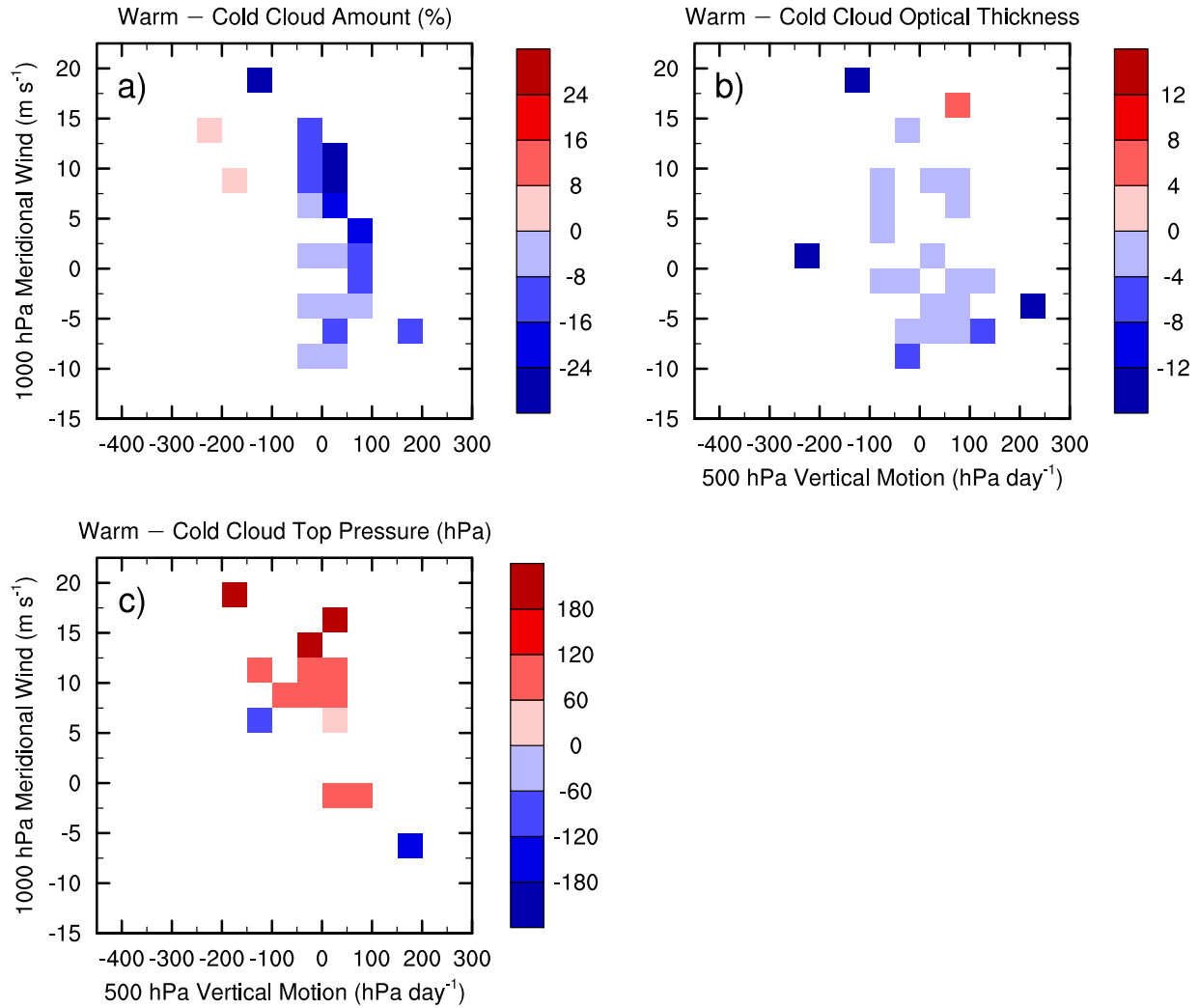


Fig. 3. As in Fig. 1, except for the average of ISCCP values associated with the lower SST and middle LTS terciles subtracted from the average of ISCCP values associated with the upper SST and middle LTS terciles. Only differences significant at the 95% level are shown.

Table 2. Average difference between upper SST/middle LTS and lower SST/middle LTS terciles.\*

Latitude Region	Cloud Amount (% K <sup>-1</sup> )	$\tau$ (K <sup>-1</sup> )	CTP (hPa K <sup>-1</sup> )	SW CRF (W m <sup>-2</sup> K <sup>-1</sup> )	LW CRF (W m <sup>-2</sup> K <sup>-1</sup> )	Net CRF (W m <sup>-2</sup> K <sup>-1</sup> )	SST anomaly (K)	LTS anomaly (K)
45-55° N	-0.1	<b>-0.7</b>	-4	+2.2	<b>+2.9</b>	<b>-4.5</b>	<b>+1.4</b>	0.0
35-45° N	<b>-2.7</b>	<b>-0.4</b>	<b>+12</b>	<b>+5.6</b>	<b>-2.4</b>	<b>-2.8</b>	<b>+2.4</b>	<b>+0.1</b>
25-35° N	<b>-5.6</b>	<b>-0.4</b>	<b>-19</b>	<b>+11.9</b>	<b>-8.2</b>	<b>-3.7</b>	<b>+1.3</b>	-0.1

\* As in Table 1. Cloud properties have been divided by the SST difference, and bold indicates differences that are significant at the 95% level.

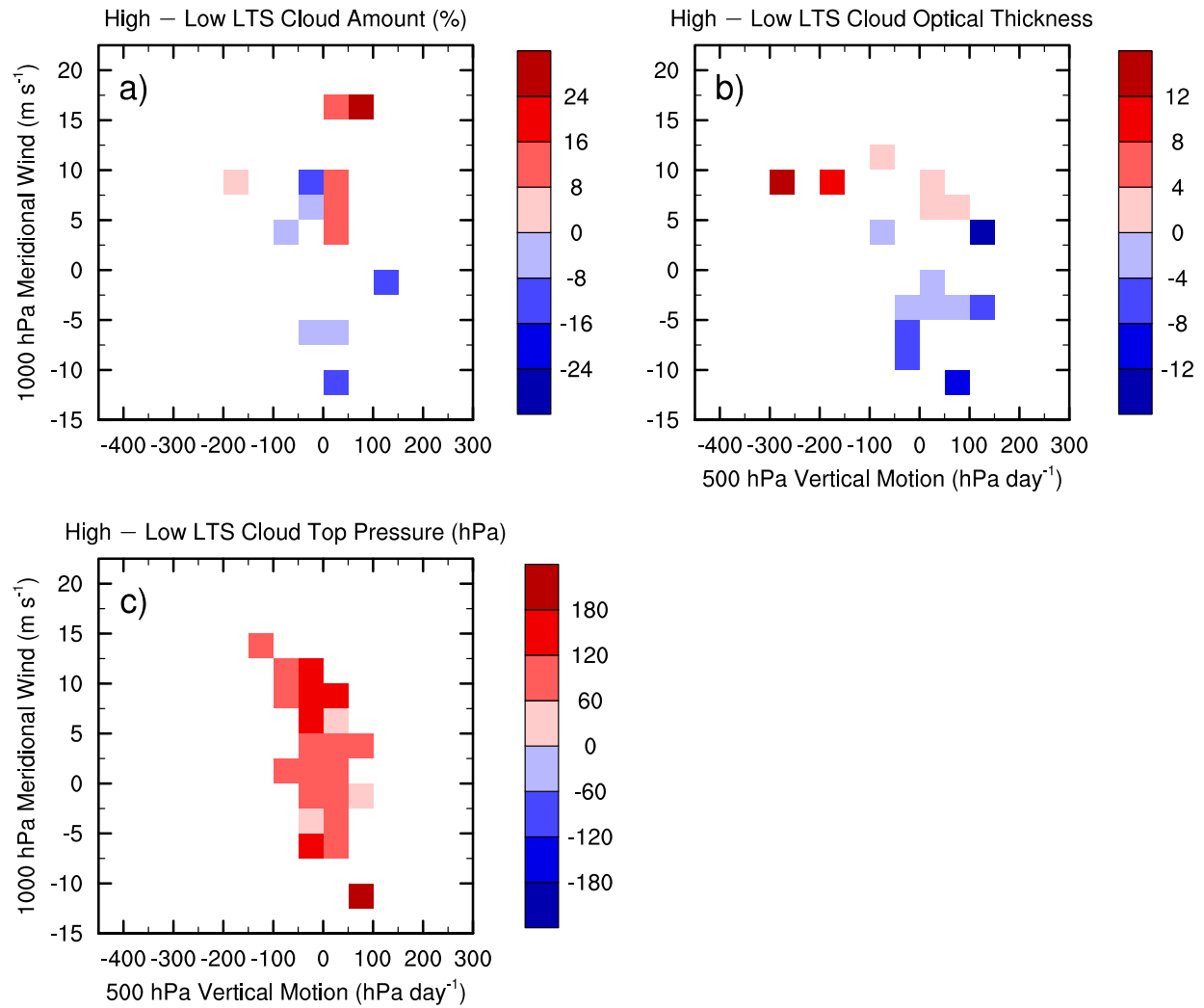


Fig. 4. As in Fig. 1, except for the average of ISCCP values associated with the middle SST and lower LTS terciles subtracted from the average of ISCCP values associated with the middle SST and upper LTS terciles. Only differences significant at the 95% level are shown.

Table 3. Average difference between middle SST/upper LTS and middle SST/lower LTS terciles.\*

Latitude Region	Cloud Amount ( $\% \text{ K}^{-1}$ )	$\tau$ ( $\text{K}^{-1}$ )	CTP ( $\text{hPa K}^{-1}$ )	SW CRF ( $\text{W m}^{-2} \text{ K}^{-1}$ )	LW CRF ( $\text{W m}^{-2} \text{ K}^{-1}$ )	Net CRF ( $\text{W m}^{-2} \text{ K}^{-1}$ )	SST anomaly (K)	LTS anomaly (K)
45-55° N	<b>-0.2</b>	<b>-0.3</b>	<b>-3</b>	<b>+2.0</b>	0.0	<b>+2.0</b>	0.0	<b>7.7</b>
35-45° N	-0.1	0.0	<b>+14</b>	<b>+2.2</b>	<b>-1.2</b>	<b>+0.8</b>	<b>-0.1</b>	<b>+4.7</b>
25-35° N	<b>-2.8</b>	<b>-0.1</b>	<b>+18</b>	<b>+3.0</b>	<b>-2.9</b>	+0.1	0.0	<b>+3.6</b>

\* As in Table 1. Cloud properties have been divided by the LTS difference, and bold indicates differences that are significant at the 95% level.

Table 4. Difference between a  $+0.1\sigma$  and a  $-0.1\sigma$  change in the standard deviation of  $\omega_{500}$  or  $\nu_{1000}$  distributions for middle SST and LTS terciles.\*

Latitude Region	Amount (%)	$\tau$	CTP (hPa)	SW CRF ( $\text{W m}^{-2}$ )	LW CRF ( $\text{W m}^{-2}$ )	Net CRF ( $\text{W m}^{-2}$ )	$\omega_{500} \Delta\sigma$ ( $\text{hPa day}^{-1}$ )	$\nu_{1000} \Delta\sigma$ ( $\text{m s}^{-1}$ )
45-55° N	-0.3	+0.2	-5	+1.5	-0.1	+1.3	+17	
35-45° N	-0.5	+0.3	-4	-2.2	+0.5	-1.7	+13	
25-35° N	+0.5	+0.2	-6	-2.2	+1.3	-0.9	+10	
45-55° N	-0.3	0.0	-2	+1.9	-0.3	+1.5		+0.7
35-45° N	0.0	+0.2	+1	+1.3	-0.5	+0.7		+0.6
25-35° N	+1.2	+0.1	+4	-1.4	+0.5	-0.9		+0.5

\*As in Table 1.  $\sigma$  is the original standard deviation of  $\omega_{500}$  or  $\nu_{1000}$  distributions, and  $\Delta\sigma$  is the difference between the modified standard deviations.

differences in Table 2 have been divided by the corresponding SST difference for purposes of comparability between different regions and time periods. As noted by previous studies of midlatitude cloud variability (e.g., Norris and Leovy 1994; Tselioudis et al. 1992; Weare 1994), warmer temperature is associated with less cloud amount and  $\tau$  in all North Pacific latitude regions, and SW CRF is correspondingly less negative. LW CRF decreases with temperature in the southern and central regions but decreases in the northern region. Net CRF is less negative for warmer conditions in all regions. Changes in the cloud fraction of individual ISCCP categories are somewhat different for each latitude region (not shown). In the southern region, warmer temperature is associated with less cloudiness by all types except optically thin high clouds. Warmer temperature in the central region occurs with substantially fewer mid- and high-level clouds and a slightly more optically thin and intermediate low-level clouds. An increase in optically thin clouds and a decrease in optically thick clouds occur at all levels for warmer temperature in the northern region.

The difference between composites for middle SST/upper LTS and middle SST/lower LTS terciles, displayed in Fig. 4 for the 35-45°N region, illustrates the response of cloud properties to changes in the stratification of the lower troposphere. Since the

correlation between 700-hPa temperature and 500-hPa (300-hPa) temperature is 0.82 (0.69), variations in LTS largely correspond to opposite changes in SST and free troposphere temperature. Similar to the case for vertically uniform warming, an increase in LTS results in higher CTP. Cloud amount and  $\tau$ , however, exhibit little overall change due to compensating increases and decreases in different dynamical regimes. Higher LTS favors a large increase in low-level cloudiness at the expense of mid- and high-level clouds (not shown). This is consistent with the existence of a shallower boundary layer that, under poleward advection, traps moisture and hastens the onset of fog formation, and that, under equatorward advection, delays the onset of decoupling and stratocumulus breakup. Table 3 lists mean differences in ISCCP and ERBE cloud properties, normalized by the corresponding LTS difference. SW CRF becomes less negative with increasing LTS in all latitude regions, and LW CRF decreases in the southern and central regions due to less mid- and high-level cloud cover.

One possible confounding factor in the preceding analyses is the meridional variation in cloud properties. Previous research by Norris (2000) documented the frequent co-occurrence of interannual shifts in the latitude of the SST gradient and in the latitude of the storm track as well as associated nimbostratus clouds. Since northward movement of the location of the SST

gradient results in a local warm SST anomaly, a coincidental movement from the south of cloudiness with different characteristics could create an apparent dependence of cloud properties on temperature. This effect is partially mitigated by the incorporation of shifts in the local dynamical distributions by the compositing on  $\omega_{500}$  and  $v_{1000}$ , but Table 2 may nonetheless overestimate the cloud change per degree warming. Unfortunately, it is very difficult to observationally distinguish changes in cloudiness directly due to temperature from meridional shifts in cloudiness indirectly related to temperature. Consequently, the results of this study will be most applicable to the question of the cloud response to global warming if the storm track and SST gradient also move poleward.

#### 4. CLOUD RESPONSE TO DYNAMICAL CHANGES

Aside from variability in thermodynamical parameters, average cloud properties can change merely in response to altered frequency distributions of  $\omega_{500}$  and  $v_{1000}$ . This effect can be explored by holding constant the “normal” SST/LTS composite cloud properties displayed in Figs. 1a-c and 2a-c while averaging them with weightings different than those displayed in Fig. 1d. Dynamical changes considered are increases or decreases in the standard deviations of the  $\omega_{500}$  or  $v_{1000}$  distributions by an increment equal to one tenth of the original standard deviation. The transformation from the original distribution to the modified distribution was identical to that for normally distributed data, but the procedure did not assume that the original data were normally distributed. Mean cloud properties resulting from altered dynamics were calculated by averaging cloud values corresponding to middle terciles of SST and LTS (Fig. 1a-c and Fig. 2) with weighting according to modified  $\omega_{500}$  or  $v_{1000}$  distributions.

Table 4 lists differences in mean cloud properties when the reduced standard deviation is subtracted from the amplified standard deviation, corresponding to an intensification of the storm track and greater frequency of large positive and negative dynamical values. Increased  $\omega_{500}$  variance produces lower CTP, higher  $\tau$ , more positive LW CRF, and more negative SW CRF in the central and southern regions because stronger ascent generates higher and thicker clouds while stronger descent has less effect on low-level cloud height and thickness. SW CRF does not become more negative in the northern region since the increase in  $\tau$  due to stronger ascent is outweighed by a decrease in the amount of relatively optically thick clouds due to stronger descent. Changes in cloud properties in response to increased  $v_{1000}$  variance are less consistent between latitude regions, and, when averaged over all regions, have opposite sign and lesser magnitude than the cloud response to  $\omega_{500}$  variance. This will cause partial cancellation if shifts in the magnitude of  $\omega_{500}$  variance and  $v_{1000}$  variance are positively correlated. The cloud response to a combination of dynamical changes was nearly the same as the sum of the individual effects of shifts in the means or standard deviations of the  $\omega_{500}$  and  $v_{1000}$  distributions.

One limitation of the previous analysis of the cloud response to shifts in distribution means and standard deviations is the arbitrary specification of the magnitudes of dynamical changes. The GCM study of Dai et al. (2001) predicts that between the 1990s and the 2090s central North Pacific temperature will increase by about 2 K and the standard deviation of 2-8 day SLP variance will decrease by about 10% ( $-0.1\sigma$ ). These trends suggest the cloud response to warming will be dominant and slightly enhanced by the weakening of the storm track. Trends in GCM cloudiness are not discussed here because Norris and Weaver (2001) found substantial deficiencies in their simulation over the summertime midlatitude North Pacific at synoptic and interannual time scales.

#### 5. DISCUSSION AND CONCLUSIONS

The differences in cloud properties associated with changes in thermodynamic and dynamic parameters are consistent with the synoptic cloud relationships. Stratocumulus cloudiness breaks up when it is advected equatorward over warmer subtropical water because the subcloud layer becomes decoupled from the cloud layer, thus inhibiting the upward flux of moisture needed to sustain the cloud deck. A warm SST anomaly additionally acts to shift the main SST gradient poleward such that cloud breakup occurs sooner. The reduction of upward moisture flux also contributes to a thinning of the cloud layer. For poleward advection, higher temperature delays the onset of fog formation and therefore maintains the regime of a smaller amount of optically thinner clouds. Cloud amount decreases with rising temperature when vertical velocity is near zero or downward, but optical thickness decreases with temperature even when vertical motion is upward. More research is needed to determine why this is so. The changes in cloud amount and optical thickness both contribute to less negative SW CRF for warmer temperature. Although LW CRF becomes less positive, the change in SW CRF is larger so net CRF also becomes less negative.

Stronger LTS is generally associated with a shallower boundary layer capped by a sharper temperature inversion (Norris 1998a). In the downward/southward quadrant, optical thickness becomes smaller when LTS becomes larger, perhaps due to thinning of the cloud layer due to a lower inversion height. Contrastingly, optical thickness increases with increasing LTS in the downward/northward quadrant due to a decrease in cirrus and increase in fog. A likely reason that stronger LTS favors more fog is that greater stratification prevents moisture from leaving the surface layer. Cloud top pressure becomes larger for stronger LTS under most dynamical conditions. Stronger LTS is associated with less negative SW CRF, less positive LW CRF, and less negative net CRF.

A change in the variance of the  $\omega_{500}$  distribution can also alter mean cloud properties as a consequence of their non-linear dependence on vertical velocity. Since cloud optical thickness and cloud top height

increase more strongly with upward motion than they decrease with downward motion, more frequently occurring strong ascent and descent will produce on average greater optical thickness and top height. The impact of greater optical thickness on SW CRF is larger than the impact of top height on LW CRF, so net CRF becomes more negative when  $\omega_{500}$  variance becomes larger. Opposite changes result from a weakening of  $\omega_{500}$  variance.

Since long-term trends are merely the accumulation of daily effects, the previously documented synoptic cloud responses to changes in temperature, LTS,  $\omega_{500}$ , and  $v_{1000}$  can be used to infer the response of summertime midlatitude oceanic clouds to global warming. The results of this study suggest that cloud amount and optical thickness will decrease over the summertime North Pacific ocean and allow more solar radiation to be absorbed by the Earth. The corresponding increase in outgoing LW radiation due to weaker LW CRF only partially compensates the SW gain; consequently, clouds in this region and season act as a positive feedback on the climate system. If the ocean warms more slowly than the atmosphere due to its greater thermal inertia, then LTS will temporarily increase, and this too will change cloud properties so as to cause a net gain of energy to the climate system. Clouds may also respond indirectly to global warming through changes in atmospheric dynamics. For example, polar amplification of global warming implies less baroclinicity and an associated weakening of the storm track, which, according to calculations in this study, will result in smaller mean optical thickness and larger mean cloud top height. The radiative effects of these changes are an increase in absorbed SW and a smaller decrease in outgoing LW, again contributing to a positive cloud feedback.

The thermodynamical and dynamical connections to cloudiness documented in this study provide strong constraints for the validation of GCM cloud simulations, and it would be particularly useful to evaluate leading models by how well they reproduce the observed relationships, thereby assessing the reliability of their predictions of cloud feedbacks and future climate change.

*Acknowledgements.* A NASA GWEC grant, NAG5-11731, supported this work. C. P. Weaver graciously provided daily ERBE data. ISCCP data were obtained from the NASA Langley Research Center Atmospheric Sciences Data Center (eosweb.larc.nasa.gov), reanalysis data from the website of the NOAA-CIRES Climate Diagnostics Center (www.cdc.noaa.gov), and SST data from the International Research Institute/Lamont Doherty Earth Observatory climate data library website (iridl.ldeo.columbia.edu).

## REFERENCES

Barkstrom, B., E. Harrison, G. Smith, R. Green, J. Kibler, R. Cess, and the ERBE Science Team, 1989: Earth Radiation Budget Experiment (ERBE) archival and April 1985 results. *Bull. Amer. Meteor. Soc.*, **70**, 1254-1262.

- Bony, S., J.-L. Dufresne, H. Le Treut, J.-J. Morcrette, and C. Senior, 2004: On dynamic and thermodynamic components of cloud changes. *Climate Dyn.*, **22**, 71-86.
- Dai, A., T. M. I. Wigley, B. A. Boville, J. T. Kiehl, and L. E. Buja, 2001: Climates of the twentieth and twenty-first centuries simulated by the NCAR Climate System Model. *J. Climate*, **14**, 485-519.
- Harrison, E. F., P. Minnis, B. R. Barkstrom, V. Ramanathan, R. D. Cess, and G. G. Gibson, 1990: Seasonal variation of cloud radiative forcing derived from the Earth radiation Budget Experiment. *J. Geophys. Res.*, **95**, 18687-18703.
- Kalnay, E., M. Kanamitsu, R. Kistler, W. Collins, D. Deaven, L. Gandin, M. Iredell, S. Saha, G. White, J. Woollen, Y. Zhu, M. Chelliah, W. Ebisuzaki, W. Higgins, J. Janowiak, K. C. Mo, C. Ropelewski, J. Wang, A. Leetmaa, R. Reynolds, R. Jenne, and D. Joseph, 1996: The NCEP/NCAR 40-year reanalysis project. *Bull. Amer. Meteor. Soc.*, **77**, 437-471.
- Norris, J. R., 1998a: Low cloud type over the ocean from surface observations. Part I: relationship to surface meteorology and the vertical distribution of temperature and moisture. *J. Climate*, **11**, 369-382.
- Norris, J. R., 1998b: Low cloud type over the ocean from surface observations. Part II: geographical and seasonal variations. *J. Climate*, **11**, 383-403.
- Norris, J. R., 2000: Interannual and interdecadal variability in the storm track, cloudiness, and sea surface temperature over the summertime North Pacific. *J. Climate*, **13**, 422-430.
- Norris, J. R., and C. B. Leovy, 1994: Interannual variability in stratiform cloudiness and sea surface temperature. *J. Climate*, **7**, 1915-1925.
- Norris, J. R., and C. P. Weaver, 2001: Improved techniques for evaluating GCM cloudiness applied to the NCAR CCM3. *J. Climate*, **14**, 2540-2550.
- Reynolds, R. W., N. A. Rayner, T. M. Smith, D. C. Stokes, and W. Wang, 2002: An improved in situ and satellite SST analysis for climate. *J. Climate*, **15**, 1609-1625.
- Ringer, M. A., and R. P. Allan, 2004: Evaluating climate model simulations of tropical cloud. *Tellus*, **56A**, 308-327.
- Rossow, W. B., and R. A. Schiffer, 1999: Advances in understanding clouds from ISCCP. *Bull. Amer. Meteor. Soc.*, **80**, 2261-2287.
- Rossow, W.B., A.W. Walker, D.E. Beusichel, and M.D. Roiter, 1996: *International Satellite Cloud Climatology Project (ISCCP) Documentation of New Cloud Datasets*. WMO/TD-No. 737, World Meteorological Organization, 115 pp. [Available at <http://isccp.giss.nasa.gov/docs/documents.html>.]
- Tselioudis, G., W. B. Rossow, and D. Rind, 1992: Global patterns of cloud optical thickness variation with temperature. *J. Climate*, **5**, 1484-1495.
- Weare, B. C., 1994: Interrelationships between cloud properties and sea surface temperatures on seasonal and interannual time scales. *J. Climate*, **7**, 248-260.
- Weaver, C. P., and V. Ramanathan, 1997: Relationships between large-scale vertical velocity, static stability, and cloud radiative forcing over Northern Hemisphere extratropical oceans. *J. Climate*, **10**, 2871-2887.